TNO innovation for life

Green Deal Validation Study: Technical Addendum Maritime CEMS

Analysis of test bed data

TNO Public ⟩ TNO 2026 R10086

18 February 2026

Mobility & Built Environment
www.tno.nl
+31 88 866 00 00
info@tno.nl

TNO 2026 R10086 – 18 February 2026

Green Deal Validation Study: Technical Addendum Maritime CEMS

Analysis of test bed data

Author(s)	P. Paschinger
Copy number	2026-STL-REP-100360153
Number of pages	29 (excl. front and back cover)
Number of appendices	1
Project name	GD2024-2025 NOx CEMS / Green Deal (VP407)
Project number	060.53601/01.11.02

Summary

This report is a supplementary to a study [1] that investigates the practical feasibility and usability of Continuous Emission Measurement Systems (CEMS) for monitoring NO_x-emissions on sea-going vessels within the context of the Dutch Green Deal.
The document at hand provides additional technical information on the performance of a CEMS of one supplier. To that end, engine testbed data using both laboratory equipment and CEMS sensors is analyzed. Key findings indicate that while CEMS sensors show good agreement with laboratory measurements for NO_x-concentrations, their accuracy is lower than required for regulatory compliance but sufficient for robust, low-maintenance monitoring. The main sources of uncertainty are related to exhaust mass flow calculations and sensor sensitivity to gas composition. Recommendations include the use of dedicated sensors and improved power measurement methods. The report highlights the need for further research on long-term sensor performance in marine environments.

Contents

Abbreviations

Abbreviation	Unit	Meaning
η_{vol}	1.0	Volumetric efficiency
ρ_{air}	kg/m^3	Density of air at 273.15 K and 101.325 kPa
ρ_{diesel}	kg/m^3	Density of diesel at 15°C
ρ_{exh}	kg/m^3	Density of diesel exhaust gas at 273.15 K and 101.325 kPa
CEMS	-	Continuous Emissions Measurement System
DF	1.0	Multiplicative deterioration Factor
EGR	-	Exhaust Gas Recirculation
EMF	-	Exhaust Mass Flow
f	1.0	Calculation factor (2-stroke: *f*=1, 4-stroke: *f*=0.5)
GHG	-	GreenHouse Gas
GUM 1995	-	Guide to the expression of Uncertainty in Measurement
IenW	-	Dutch Ministry of Infrastructure and Water Management
ISM	-	In-Service Monitoring
IWA	-	Auxiliary engine for Inland Waterway vessels
IWP	-	Propulsion engine for Inland Waterway vessels
MAP	bar	Manifold Air Pressure
MAT	°C	Manifold Air Temperature
n	RPM	Engine speed
NRMM	-	Non-Road Mobile Machinery
NRSC	-	Non-Road Steady-state test Cycle
NTE	-	Not To Exceed
ODR	-	Orthogonal Distance Regression
PEMS	-	Portable Emissions Measurement Systems
SCR	-	Selective Catalytic Reduction
SD	-	Speed density
SFC	g/kWh	Specific Fuel Consumption
u_{CO}	1.0	Component specific factor or ratio between densities of gas component and exhaust gas (CO)
u_{CO2}	1.0	Component specific factor or ratio between densities of gas component and exhaust gas (CO_2)
u_{NOx}	1.0	Component specific factor or ratio between densities of gas component and exhaust gas (NO_x)

1 Introduction

In the course of the Green Deal Validation program of the Dutch Ministry of Infrastructure and Water Management (IenW) technologies, which aim at the reduction of Greenhouse Gas (GHG) or pollutant emissions of maritime vessels, are validated by independent research institutions. The report at hand deals with the opportunities that are offered by the installation of Continuous Emission Measurement Systems (CEMS). To that end, the specifications of a NO_x-sensor and the data of two test-bed tests were analyzed. During both tests, laboratory equipment as well as a CEMS by Multronic N.V. (hereinafter referred to as Multronic) were used to measure the concentrations of NO_x in the exhaust gas and to determine the brake-specific NO_x emissions over the applicable test cycles and additional load points. The engine that was studied was certified acc. to Stage V standards [2], [3], [4]. The first test was for an auxiliary engine for inland waterway vessels with constant speed of 1500 RPM and a rated power of 599 kW (IWA-c-4). The applicable Non-Road Steady-state test Cycle (NRSC) according to [5], [6] is D2. The exact category of the second test is not mentioned in the information provided to TNO but is either Propulsion engine for Inland Waterway vessels (IWP) or IWA. The variable engine speed and the rated power of 599 kW yield either category IWP-v-4 or IWA-v-4. The applicable NRSC is E3. The regulated maximum brake-specific NO_x-emissions for both engine categories are stated in Table 1.1 below. For all engines for inland waterway vessels with a rated power of more than 300 kW, 1.80 g/kWh apply independent of the usage as propulsion or auxiliary engine and whether the engine spins at constant or variable speed.

Table 1.1: NO_x-emission limits for selected engine sub-categories (cf. [4])

Emission stage	Engine sub-category	Power range	Ignition type	NO_x [g/kWh]
Stage V	IWA-c-4 IWA-v-4	≥ 300 kW	all	1.80
Stage V	IWP-c-4 IWP-v-4	≥ 300 kW	all	1.80

The composition of the D2 and E3 test cycles as well as the weighting factors per mode are stated in Table 1.2 below. An important difference between the two cycles is that only D2 has a 10 % load point whilst the minimum load for E3 is 25 %. In general, higher weighting factors are applied at higher load points in the E3 cycle.

Table 1.2: D2 and E3 test cycles according to [5], [6]

Test Cycle	Parameter	Mode 1	Mode 2	Mode 3	Mode 4	Mode 5
D2	Speed	100 %	100 %	100 %	100 %	100 %
	Power	100 %	75 %	50 %	25 %	10 %
	Weighting factor	0.05	0.25	0.3	0.3	0.1
E3	Speed	100 %	91 %	80 %	63 %	n/a
	Power	100 %	75 %	50 %	25 %	n/a
	Weighting factor	0.2	0.5	0.15	0.15	n/a

The aim of this study is to evaluate the suitability of CEMS for monitoring of NO_x-emissions of seafaring vessels. However, only testbench data and no long-term onboard measurement data were available. Therefore, the scope of this study and of the conclusions is limited.

The research questions that were studied were:

1. What are the sources of uncertainty of the CEMS compared to laboratory equipment?
2. How large are the contributions of the different sources to the total measurement uncertainty?

2 Methods

The analysis of this study is based on data that origins from two testbed measurements of an engine for inland waterways rather than on long-term onboard monitoring data of seafaring vessels. The first test was a D2-cycle test with an additional NTE test. The second test applied an E3-cycle and two additional load points. During both tests, the Multronic sensors and the laboratory equipment measured in parallel. A sketch of the setup of the Multronic system can be found in Figure 4.1 in annex A.4. However, only for the D2-test the final results of the certification report were made available to TNO. Furthermore, Multronic shared a spec sheet of the installed type of NO_x-sensor. An overview of the information provided by Multronic is given in annex A.1.

Python was used for the analysis of the above data. Since the data of the laboratory equipment had been logged at 10 Hz, it had to be resampled to 1 Hz to allow for direct comparison of time stamps. For further analysis, the last value of a bin was used because this aggregation also works for non-numeric data types. During resampling of data to a lower sampling frequency information is lost which leads to small deviations in the final results. However, since only steady state operations are considered in the D2- and E3-tests, respectively, and 1 Hz is the minimum recording frequency for type approval tests of Non-Road Mobile Machinery (cf. [3, Tbl. 6.7]), the additional uncertainty is acceptable.

The time-alignment of Multronic and laboratory data was done manually based on the logged values of engine power. Since only steady-state data was analysed, the impact is negligible. The aligned signals can be found in Figure 3.1 and Figure 3.7 in section 3.2.

In the Multronic data, the exhaust volume flow at normal conditions (column **QIn [l/s]**) had been calculated by applying the so-called speed-density (SD) method. The formula is stated in Equation 2.1 below. A description of the symbols can be found in the Abbreviations section on page 6. The values of the volumetric efficiency η_{vol} were obtained by interpolation of a map that provided volumetric efficiency as a function of engine speed and MAP. For the calculation of NO_x mass emissions from exhaust volume flow, the parameters given in [3] were used. The values are stated in Table 4.1 in annex A.2.

Equation 2.1: Speed-density method.

$$\dot{V}_{\mathrm{n}} = \eta_{\mathrm{vol}} \cdot f \cdot V_{\mathrm{disp}} \cdot \frac{n}{60} \cdot \frac{273.15}{\mathrm{MAT} + 273.15} \cdot \frac{\mathrm{MAP}}{1.01325}$$

Since the exhaust mass flow is a main driver of measurement uncertainty, the error propagation and error amplification (relative numeric condition) of Equation 2.1 will be studied in detail.

3 Results

3.1 Analysis of accuracy

3.1.1 Specifications and requirements

Commission Delegated Regulation 2017/655 [2] requires Portable Emissions Measurement Systems (PEMS) that are to be used for the monitoring of gaseous pollutant emissions from in-service internal combustion engines installed in non-road mobile machinery to meet the specifications set out in Section 9.4 of Annex VI to Delegated Regulation (EU) 2017/654 [3]. The accuracy requirements for continuous gas analysers set out there are given in Table 3.1 below. To assess the suitability of CEMS for monitoring, these values were taken as a reference and compared to the accuracy of the NO_x concentration measurement according to the spec sheet as given in Table 3.2. The rise time[1] is stated in the spec sheet to be between 0.6 and 1.8 seconds.

Table 3.1: Recommended performance specifications for measurement instruments [3, Tbl. 6.8].

Measurement Instrument	Measured quantity symbol	Complete System Rise time	Recording update frequency	Accuracy[2]	Repeatability[2]
Continuous gas analyzer	x	5 s	1 Hz	2.0 % of pt. or 2.0 % of meas.	1.0 % of pt. or 1.0 % of meas.

Table 3.2: Accuracy of Multronic NO_x sensor acc. to spec sheet.

NO-concentration	Fresh	Aged
0 ppm	± 8 ppm	± 10 ppm
90 ppm	± 10 ppm	± 12 ppm
1500 ppm	± 8 %	± 10 %

The accuracy of fresh sensors does not fulfil the recommendations of [3] and decreases when the sensor ages – which is relevant for long-term monitoring applications. The rise time is much lower than the one stated in Table 3.1. This comparison does, however, not necessarily mean that the sensor is not suited for long-term monitoring since the goal and therefore the requirements on sensors are different to In-Service Monitoring (ISM) where accurate measurements are needed to assess the compliance of machinery.

3.1.2 Calculation of exhaust (mass) flow

The determination of exhaust mass flow significantly contributes to the overall uncertainty of the measured emitted mass of NO_x.

[1] In the spec sheet the difference in time between the 10 percent and 90 percent response of the final reading is referred to as "Response time NO".

[2] "pt." refers to the overall mean value expected at the emission limit
"meas." refers to the actual mean measured over the duty cycle.

The Guide to the expression of Uncertainty in Measurement (GUM 1995) [7] defines the combined standard uncertainty u_c of a measurand that is obtained from N independent quantities through a functional relationship f as the square root of the combined variance stated in Equation 3.1 below.[3]

Equation 3.1: Combined standard uncertainty acc. to [7, p. 19].

$$u_c^2 = \sum_{i=1}^{N} \left(\frac{\partial f}{\partial x_i}\right)^2 \cdot u_i^2(x_i)$$

In this equation, the $u_i^2(x_i)$ refer to the variances of the different input quantities. If f is identified with the relationship of the SD-method given in Equation 2.1, the partial derivatives are as follows:

Equation 3.2: Partial derivatives of SD-formula (Equation 2.1).

$$\frac{\partial \dot{V}_\mathrm{n}}{\partial n} = \eta_\mathrm{vol} \cdot f \cdot V_\mathrm{disp} \cdot \frac{1}{60} \cdot \frac{273.15}{\mathrm{MAT} + 273.15} \cdot \frac{\mathrm{MAP}}{1.01325}$$

$$\frac{\partial \dot{V}_\mathrm{n}}{\partial \eta_\mathrm{vol}} = f \cdot V_\mathrm{disp} \cdot \frac{n}{60} \cdot \frac{273.15}{\mathrm{MAT} + 273.15} \cdot \frac{\mathrm{MAP}}{1.01325}$$

$$\frac{\partial \dot{V}_\mathrm{n}}{\partial \mathrm{MAT}} = -\eta_\mathrm{vol} \cdot f \cdot V_\mathrm{disp} \cdot \frac{n}{60} \cdot \frac{273.15}{(\mathrm{MAT} + 273.15)^2} \cdot \frac{\mathrm{MAP}}{1.01325}$$

$$\frac{\partial \dot{V}_\mathrm{n}}{\partial \mathrm{MAP}} = \eta_\mathrm{vol} \cdot f \cdot V_\mathrm{disp} \cdot \frac{n}{60} \cdot \frac{273.15}{\mathrm{MAT} + 273.15} \cdot \frac{1}{1.01325}$$

Note that correct units have to be used when the partial derivatives are evaluated. Clearly, the combined uncertainty depends on the current operating conditions and is, for example, higher for higher manifold air pressures when all other input parameters are kept constant. It has to be noted that the combined standard uncertainty calculated from Equation 3.1 represents an absolute value. Rising uncertainty does therefore not necessarily mean that the quality of the measurements decreases. The relative difference between reading and true flow may not change. A parameter that describes the propagation of relative errors to input parameters is the relative partial condition number defined by

Equation 3.3: Relative partial condition number.

$$\kappa_{\mathrm{rel,hk}} := \frac{\left|\frac{\partial f_k(\mathbf{x})}{\partial x_h}\right| \cdot |x_h|}{|f_k(\mathbf{x})|} \quad h = 1 \ldots \mathrm{m}, k = 1 \ldots \mathrm{n}$$

where f_k refers to a k-dimensional functional relationship between h input parameters. In case of the SD-method, f is only one-dimensional. The calculation of the partial condition numbers with respect to the different input quantities can be found in Equation A.1 in annex A.3. Since all of them are equal to unity or lower, relative errors in the inputs will not be amplified by applying Equation 2.1 which leads to reliable results over a wide range of input parameters.

[3] This is based on the assumption that the input quantities are uncorrelated which is approximately the case for the quantities used in the SD-method. It is assumed that the impact of MAP on the volumetric efficiency is negligible.

The SD-method is impacted by the use of Exhaust Gas Recirculation (EGR). Despite the slightly different properties of exhaust gas compared to intake air and the raised temperatures and pressures at the intake manifold, recirculating exhaust gas from the cylinders affects the time alignment of EMF and measured concentration which might cause deviations in highly dynamic conditions. Since such conditions are not typical for maritime applications, the impact on long-term NO_x monitoring onboard seafaring vessels might be limited.

3.2 Analysis of testbed data

In this section the data of the two testbed measurements are analyzed and the differences between the CEMS and the laboratory equipment are studied.

3.2.1 D2-cycle: Constant-speed auxiliary engine

The data on the D2-cycle is dealt with first because for this test the results reported for the certification were available and could serve as a reference for the outcome of the analysis. The reported brake-specific emissions for the different modes of the cycle and the NTE-point are stated in Table 3.4 below. The table also includes the numbers for NO_x, CO, and CO_2 that were obtained from the laboratory measurement equipment. The applied deterioration factors can be found in Table 3.3.

Table 3.3: Deterioration factors.

	NO_x	CO_2	CO
DF (multiplicative)	1.15	1.0	1.30

Table 3.4: D2-cycle reference results.

Mode	NO_x [g/kWh]	CO_2 [g/kWh]	CO [g/kWh]
Mode 1	0.565	635.7	0.047
Mode 2	0.522	648.9	0.035
Mode 3	0.637	667.5	0.025
Mode 4	0.451	737.6	0.026
Mode 5	8.642	951.3	0.017
NTE	0.441	648.8	0.036
Test results (w/o DF)	0.723	673.9	0.031
Final results w/ DF	0.831	673.9	0.040

The results calculated by TNO during the analysis are stated in Table 3.5 below. In addition to brake-specific emissions of NO_x, CO, and CO_2 of the laboratory equipment, there is also a column that summarizes the results based on the CEMS data.

Table 3.5: D2-cycle emission results of this study.

Mode	Laboratory			CEMS
	NO_x [g/kWh]	CO_2 [g/kWh]	CO [g/kWh]	NO_x [g/kWh]
Mode 1	0.557	629.4	0.047	0.532
Mode 2	0.518	645.2	0.035	0.519
Mode 3	0.626	664.5	0.025	0.561
Mode 4	0.437	734.3	0.026	0.375
Mode 5	8.592	946.2	0.017	5.048
NTE	0.437	644.3	0.035	0.425
Test results (w/o DF)	0.714	670.1	0.031	0.652
Final results w/ DF	0.821	670.1	0.041	0.750

First, the agreement of the calculated laboratory values with the ones stated in the test report is discussed in order to verify that the method has been applied correctly. With respect to NO_x, there is no clear trend towards lower or higher brake-specific emissions that applies for all modes. The maximum absolute difference between the NO_x emissions determined by laboratory measurement equipment occurred in Mode 5 and was -50 mg/kWh which is equivalent to -0.6% of the reference. For the total D2-cycle, the difference is -10 mg/kWh and -1.2 %. The relative difference for the brake-specific CO_2-emissions is less than ±1.0 %, which gives confidence that the calculation method applied by TNO sufficiently reproduces the results of the certification report. The maximum difference between the results for CO is 1.0 mg/kWh. Due to the low absolute values, this led to a relative difference of 1.9 %. Overall, the differences are tolerable and can be explained by the effect of resampling the data at 1 Hz and truncation errors.

Turning to the difference between the two NO_x-columns of Table 3.5, one realizes that the reference results are always higher than the ones calculated based on CEMS data. The relative difference between the final results is -8.6 %. In the case of Mode 5, the difference is more than 3500 mg/kWh or 41 % of the laboratory reference. The two main drivers of this difference can be seen in Figure 3.1 and Figure 3.4. According to the former, the engine power used by CEMS was significantly higher than the one used in the reference calculation. The latter figure shows that, particularly in Mode 5, the measurements of NO_x concentration differ. Both plots will be discussed in more detail later in this section.

Table 3.6 provides an overview of the total work and mass emissions per mode determined by the laboratory equipment and CEMS. Not that the NTE mode is not included in the final results, which only represents the totals over the test cycle. The total mass flow as determined based on CEMS was 0.3 % higher. The relative differences in engine work range from 1.3 % at high engine load to 64.7 % at low engine load, with a difference of total cycle work of 8.2 %.

Table 3.6: D2-cycle exhaust mass and work of this study.

Mode	Laboratory		CEMS	
	Exhaust mass [kg]	Work [kWh]	Exhaust mass [kg]	Work [kWh]
Mode 1	107.6	22.2	107.3	22.5
Mode 2	86.6	16.6	87.4	17.3
Mode 3	66.6	11.0	66.2	12.1
Mode 4	50.9	5.5	52.0	6.7
Mode 5	44.4	2.2	44.2	3.6
NTE	87.2	16.8	87.9	17.5
Final results	356.1	57.5	357.0	62.3

The power signals used for time-alignment and for the determination of engine work are depicted in Figure 3.1 below. The different signals are labelled by using a naming convention that will be maintained throughout the entire report: Information obtained from the CEMS is labeled as 'CEMS' whilst the signals from the laboratory measurement equipment are referred to as 'Lab'. Derived data that has been calculated based on one of the sources is prefixed by 'TNO'. Data from the two sources was deliberately not combined so that it remains possible to obtain calculated results from only CEMS data in future applications where no parallel laboratory measurement takes place. The course of the three timeseries shows that the time-alignment worked sufficiently well. Furthermore, the load points of the D2-cycle are clearly visible. The rightmost step in the signals represents the additional NTE-point which is not part of the D2-cycle and has not been considered in the determination of the brake-specific emissions over the cycle. Apparently, the NTE-point is close to Mode 2, which is supported by the similar brake-specific CO_2 emissions of these two modes.
The engine power in 'Lab' shows good agreement with the nominal setpoints of the dynamometer. The power used by CEMS is generally higher. A possible reason is that signals from the engine's CAN-bus were used that represent indicated power rather than shaft power. If a SFC map and the instantaneous FC were used to determine power, the power demand of auxiliaries might as well lead to an overestimation of shaft power.

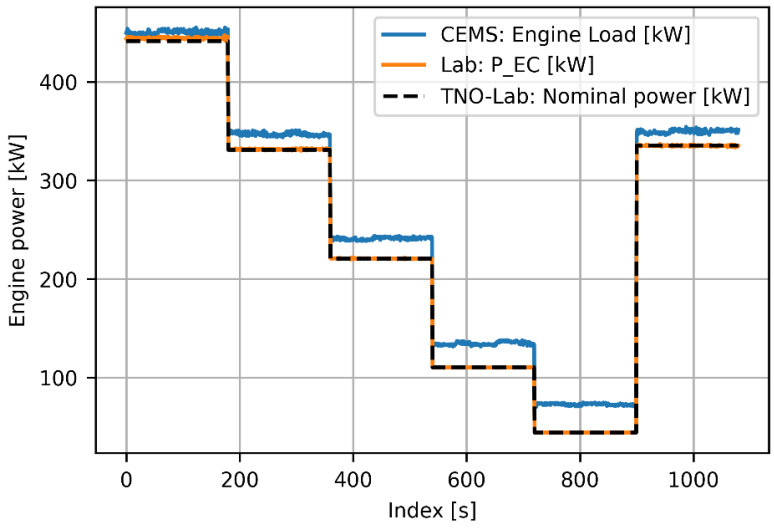

Figure 3.1: Comparison of engine power signals (D2-cycle and one NTE-point).

Figure 3.2 contains a scatter plot of the two power signals used in the evaluation of the test. A fit based on Orthogonal Distance Regression (ODR) shows a good correlation of the results. The offset of 31.38 kW might be caused by the power consumption of engine auxiliaries and parasitic losses.

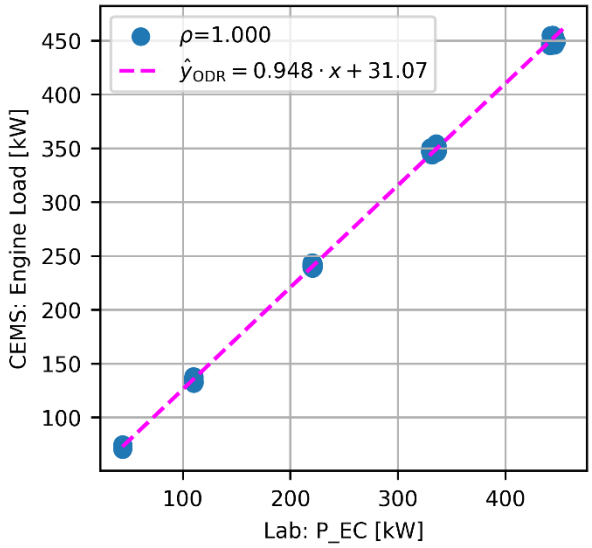

Figure 3.2: Scatter plot of engine power signals (D2-cycle and one NTE-point).

As has been mentioned before, EMF has a significant impact on the determination of brake-specific mass emissions of pollutants and greenhouse gases. Therefore, the EMF-data used to determine the results listed in Table 3.5 are compared in the scatter plot in Figure 3.3. Note that both time series have been calculated by TNO because they were not readily available in the raw data. Again, the correlation is very good with a gain close to unity and an offset that is practically zero. Therefore, the uncertainty in the final NO_x mass-emissions that can be attributed to the determination of EMF is negligible in this test.

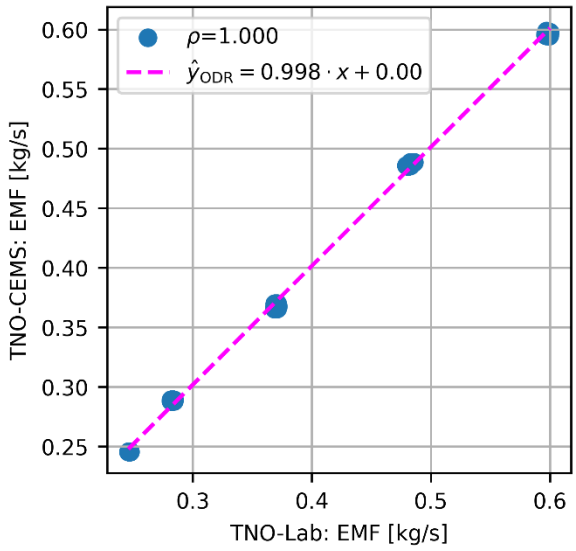

Figure 3.3: Comparison of EMF (D2-cycle and one NTE-point).

The course of NO_x-concentration signals shown in Figure 3.4 has already been mentioned briefly. It shows the course of the concentrations of NO_x (left ordinate) and CO_2 (right ordinate). For the reference (laboratory) measurement equipment, the concentrations of NO and NO_2 were available separate from each other and were added to the plot as well. Again, the different load points can be clearly identified based on, for example, the concentration of CO_2 in the exhaust gas. The rightmost part with raised CO_2-concentration is the NTE-point (close to Mode 2).

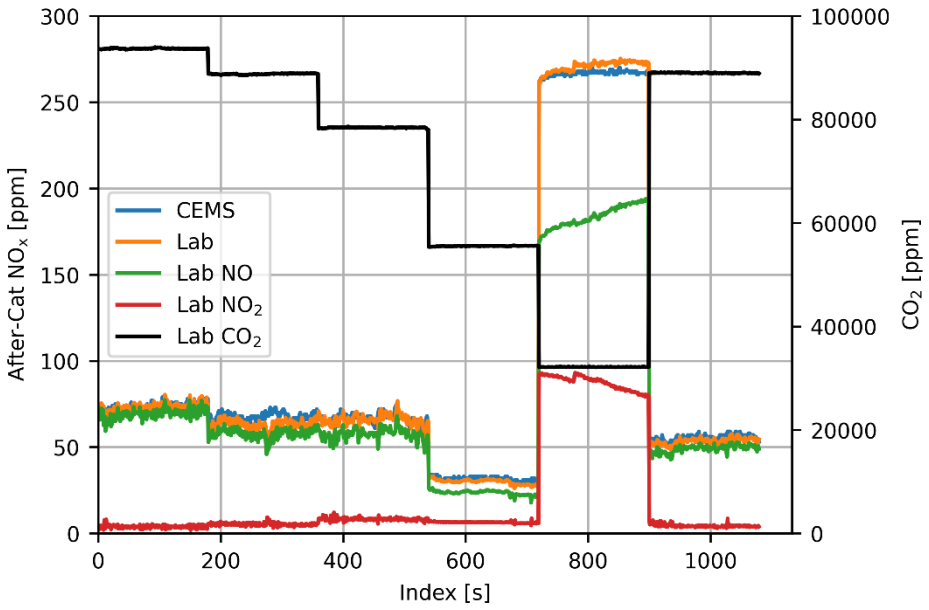

Figure 3.4: Concentrations of NO, NO_2, NO_x, and CO_2 (D2-cycle and one NTE-point).

For engine loads between 75 % and 50 % (Modes 2 and 3), there is no big step in the NO_x-signal. At 25 % engine load the NO_x-concentrations are significantly lower to rise to almost four times the concentration of Mode 1 at 10 % engine load. The latter might be the consequence of a reduced efficiency of the SCR. Except for Mode 5, the concentration of NO_2 in the exhaust gas was almost constant. The raised level of NO_2 in the low-load mode might also be caused by changes in the working of the SCR. It can also be seen that the ratio NO/NO_2 changed during Mode 5 towards a higher share of NO while the NO_x-concentration was almost constant. The fact that the CEMS logged significantly lower concentrations of NO_x compared to the laboratory equipment in Mode 5 might be attributed to a lower sensitivity to NO_2 of the CEMS sensor.

Since electrochemical NO_x-sensors are known to have different response to NO_2 compared to NO, the average readings per mode of the CEMS NO_x sensor are shown together with the average share of NO_2.

Table 3.7: D2-cycle NO_2 share and NO_x reading.

Mode	NO_2 share [%]	Rel. deviation of CEMS NO_x reading [%]
Mode 1	5.3	0.7
Mode 2	8.5	7.7
Mode 3	12.5	1.2
Mode 4	21.3	5.3
Mode 5	32.3	-1.5
NTE	8.2	4.1

Based on the data shown in Figure 3.3 and Figure 3.4 the mass flow of NO_x was calculated and the results are depicted in Figure 3.5 below. The correlation is again very good, the gain, at practically zero offset, indicates an underestimation by the CEMS which aligns with the final results shown in Table 3.5.

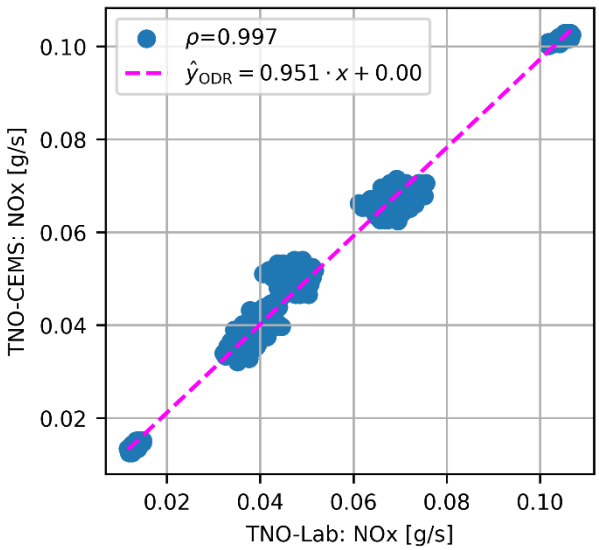

Figure 3.5: Comparison of NO_x mass flow (D2-cycle and one NTE-point).

In a last step, the variance of the NO_x-concentration readings over time were studied per mode. The results are shown in Figure 3.6. For every mode, the readings were binned into bins with a width of 1 ppm. Furthermore, the sample means and standard deviations of the modes were determined and normal distributions based on these numbers were added to the plots. Comparing the means supports the findings discussed at Figure 3.4, particularly that the difference between the two instruments is significant in Mode 5. The widths of the confidence intervals around the means indicate that the averaging time of three minutes was sufficient to obtain a statistically sound average per bin. Interestingly, Mode 5 is the mode with the lowest noise (standard deviation) both absolute and relative.

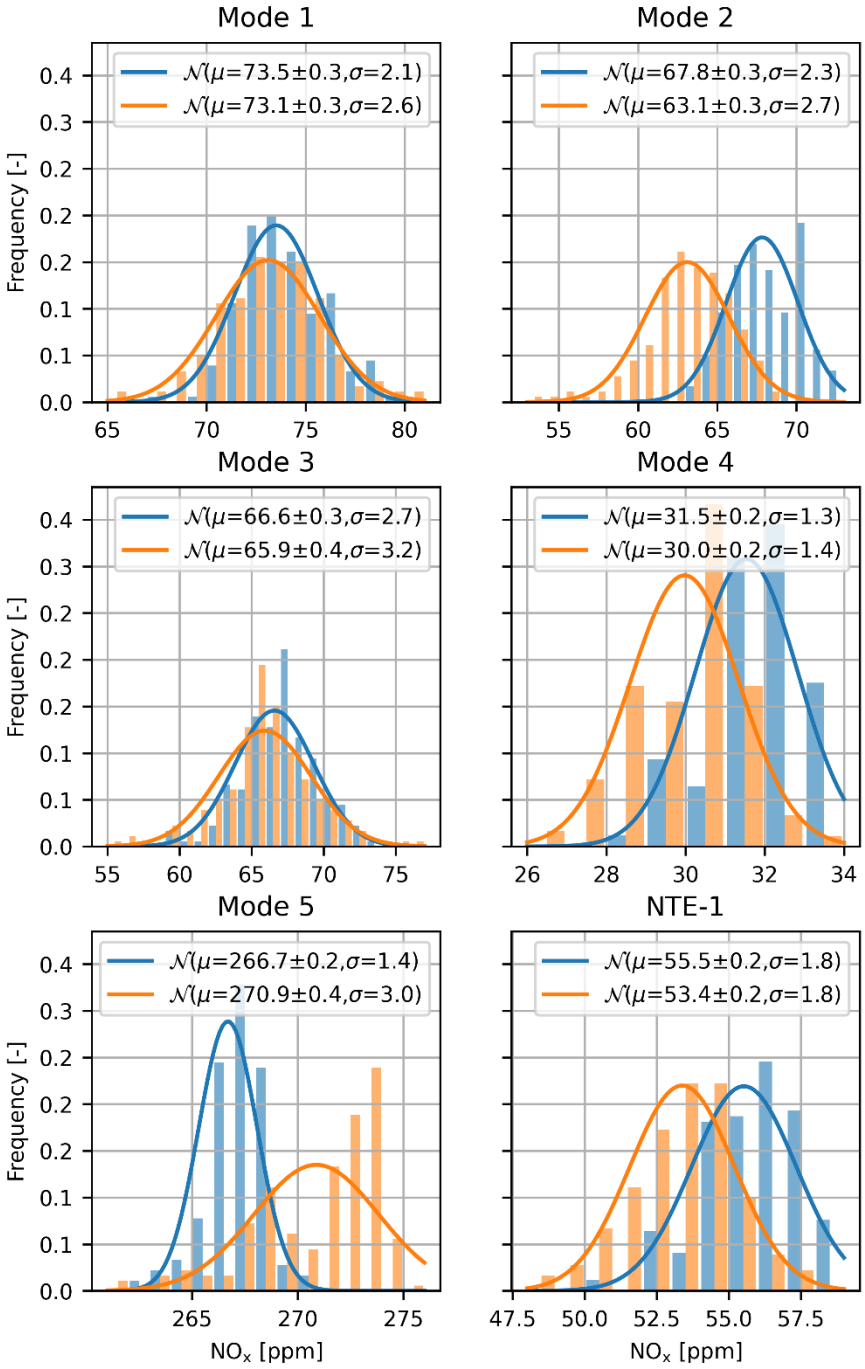

Figure 3.6: Comparison of variances of NO_x-concentration measurement (D2-cycle and one NTE-point).

3.2.2 E3-cycle: Propeller-law-operated main and propeller-law-operated auxiliary engine

In this section the findings based on the second set of data, an E3-cycle and two random load points, are discussed. Unfortunately, the reported results were not available for this data. As a consequence, the results for CO_2 and CO are only informative and could not be used to verify the calculation method.

However, since the format of the data was identical to the one used for the D2-cycle and the validation was positive for this one, it is assumed that also the results for the E3-cycle stated in Table 3.5 are valid.

Unlike the previous test, there is no clear trend of the CEMS towards over- or underestimating the brake-specific NO_x-emissions. The relative difference of the final result is about -1.4 %, in Mode 3 – the worst-case – it is -17.1 %.

Table 3.8: E3-cycle emission results of this study.

Mode	Laboratory			Multronic
	NO_x [g/kWh]	CO_2 [g/kWh]	CO [g/kWh]	NO_x [g/kWh]
Mode 1	1.025	668.4	0.018	1.015
Mode 2	1.217	616.2	0.011	1.223
Mode 3	1.279	625.8	0.009	1.234
Mode 4	1.285	649.8	0.006	1.065
Rand. load point 1	1.555	621.2	0.009	1.491
Rand. load point 2	1.042	629.6	0.013	1.060
Test results (w/o DF)	1.171	634.3	0.013	1.155
Final results w/ DF	1.347	634.3	0.016	1.328

Table 3.9 provides an overview of the total work and mass emissions per mode determined by the laboratory equipment and CEMS. Not that the two random load points are not included in the final results. The total mass flow as determined based on CEMS was 0.3 % higher. The relative differences in engine work range from -1.2 % at high engine load to 11.3 % at low engine load. The total cycle works differ by 1.2 %.

Table 3.9: E2-cycle exhaust mass and work of this study.

Mode	Laboratory		CEMS	
	Exhaust mass [kg]	Work [kWh]	Exhaust mass [kg]	Work [kWh]
Mode 1	183.6	29.6	181.6	29.3
Mode 2	141.7	22.1	142.4	21.7
Mode 3	88.7	14.6	89.5	15.3
Mode 4	46.1	7.2	47.7	8.0
Rand. load point 1	112.1	17.3	109.7	17.3
Rand. load point 2	156.7	22.7	156.6	22.1
Final results	460.2	73.5	461.2	74.3

Time-alignment and engine load comparison is shown in Figure 3.7. The power signal used by the CEMS seems to underestimate power at high engine loads and to overestimate it at low loads. Furthermore, there is less noise during the latter. These findings are supported by the scatter plot and the fit in Figure 3.8. The offset of 25.84 kW most likely represents internal engine losses and auxiliary power consumption.

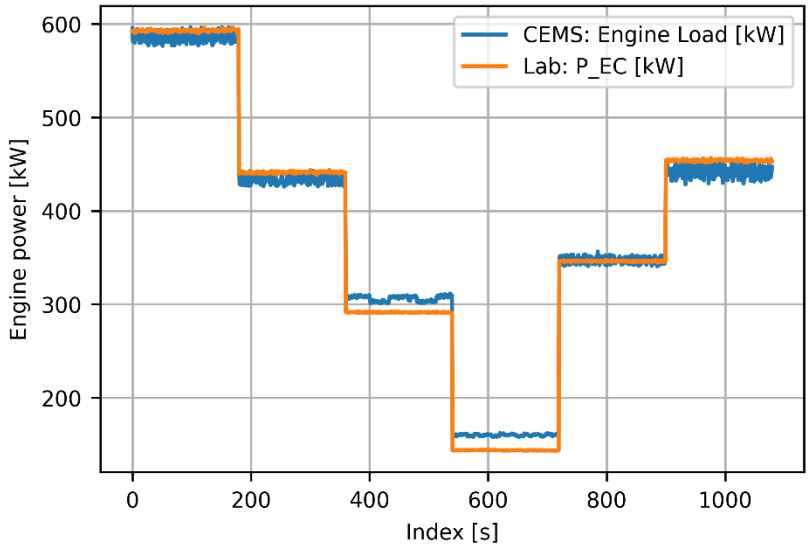

Figure 3.7: Comparison of engine power signals (E3-cycle and two random load points).

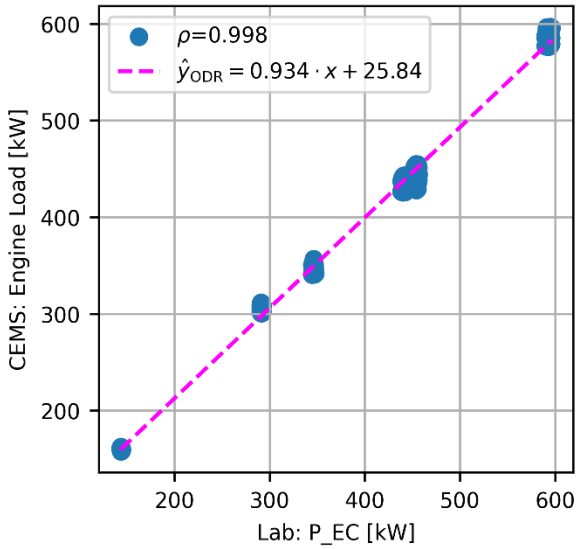

Figure 3.8: Scatter plot of engine power signals (E3-cycle and two random load points).

The calculated EMF signals are show in Figure 3.9 below. At low EMF, the CEMS values are higher whilst at higher flows, the impact of the gain outweighs the offset and yields an underestimation by the CEMS.

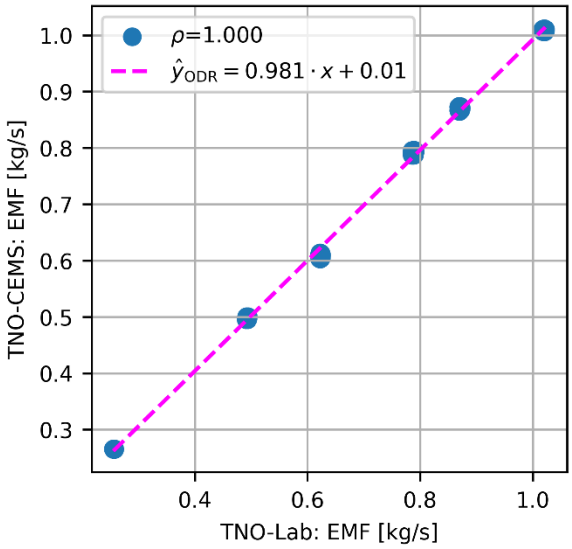

Figure 3.9: Comparison of EMF (E3-cycle and two random load points).

The course of NO_x- and CO_2-concentrations are depicted in Figure 3.10 below. For the reference instrument also NO and NO_2 were added. The signals show higher noise levels than the ones in Figure 3.4. The reason for this is unknown but since this applies for all signals in Figure 3.10, it is most probably due to actual changes in engine operation or the working of the aftertreatment systems. Interestingly, the concentration of CO_2 in Mode 2 is the lowest of the four modes of the E3-cycle. Since CO_2 mass emissions correlate with fuel consumption and therefore with engine power, one would expect that the CO_2 mass flow of Mode 2 lies between the ones of Mode 1 and Mode 3. This is actually the case. There are several possible reasons why this does not apply for the concentration of CO_2 in the exhaust gas. The most important is the disproportionally lower EMF in higher modes (lower load). The main reason for this behavior is the reduced engine speed that follows a propeller-law. Furthermore, there might be a wastegate installed in the engine that limits air intake at maximum power but not at 75 % load. In addition, the specific fuel consumption of Mode 2 might be closer to the sweet spot of the SFC-map than is the case in the other modes. NO_x levels are generally higher than has been observed in Figure 3.5 and increase towards lower load points. As has been the case in Figure 3.5, the CEMS tends to underestimate NO_x concentration when the NO/NO_2-ratio is lower, cf. Table 3.10. In Figure 3.10 this is particularly the case in Mode 4.

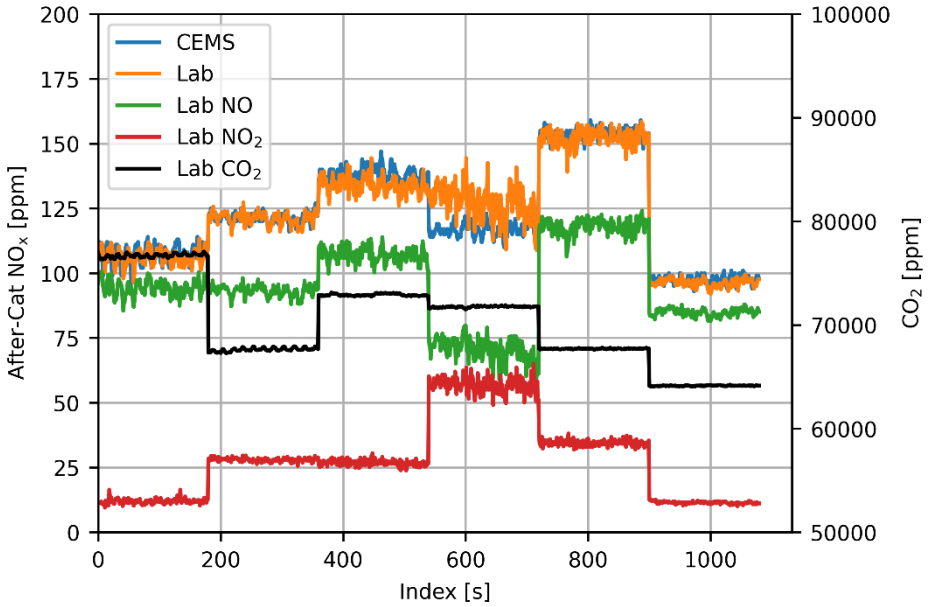

Figure 3.10: Concentrations of NO, NO_2, NO_x, and CO_2 (E3-cycle and two random load points).

Table 3.10: E2-cycle NO_2 share and NO_x reading.

Mode	NO_2 share [%]	Rel. deviation of CEMS NO_x reading [%]
Mode 1	11.3	1.0
Mode 2	23.1	0.3
Mode 3	20.0	3.0
Mode 4	44.6	-8.0
Rand. load point 1	22.6	0.9
Rand. load point 2	11.9	1.1

The NO_x mass flows are compared in Figure 3.11. The correlation is good, gain is close to unity, and the offset is practically zero. The values are higher Compared to the D2-cycle.

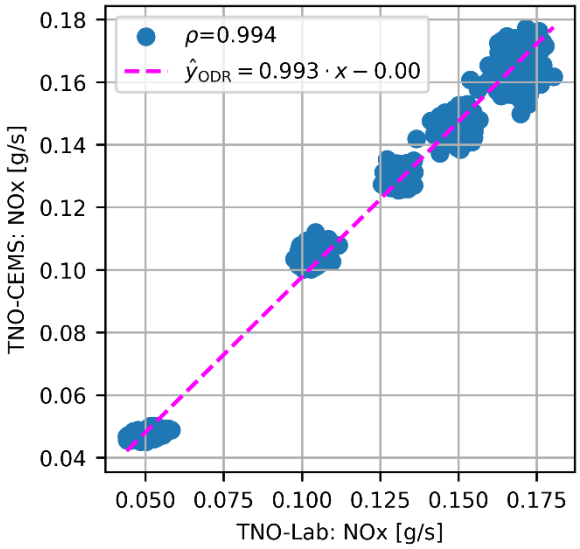

Figure 3.11: Comparison of NO_x mass flow (E3-cycle and two random load points).

The detailed analysis of the NO_x-concentration readings shown in Figure 3.12 quantifies the high levels of noise observed in Figure 3.10. The differences in sample means are small but, in many cases, significant. The application of a correction might be possible to improve the results of long-term monitoring. However, this approach would require a model and calibration of the sensor for the application and therefore increase the effort for the monitoring system and pose a source of error.

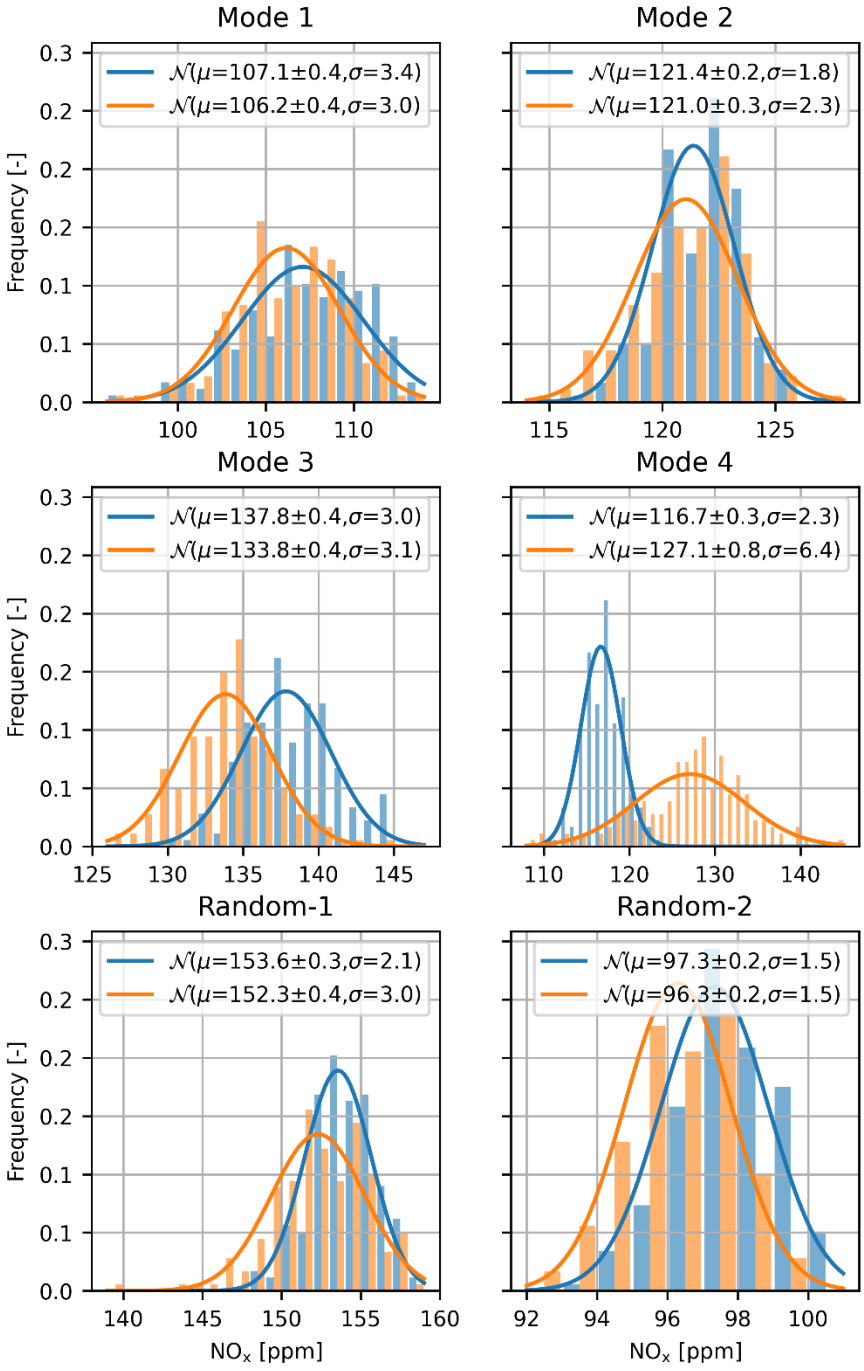

Figure 3.12: Comparison of variances of NO_x-concentration measurement (E3-cycle and two random load points).

4 Discussion and conclusion

The research described in this study showed that the accuracy of the NO_x sensor is worse than what would be required for In-Service Monitoring. However, the requirements for long-term monitoring are different since the focus is more on robust and reliable measurements that require little maintenance rather than on high accuracy.

Analysis of testbed data showed good agreement of CEMS-sensors and laboratory equipment with regard to the concentration of NO_x. The sensitivity of the NO_x reading to NO/NO_2 ratio and the concentration of ammonia (originating from the SCR) is an issue that could be addressed by installing dedicated NH_3/NO_2 sensors which are commercially available for automotive applications, or by applying correction factors based on engine models. Engine power and exhaust mass flow are also relevant sources of uncertainty that affect the determination of brake-specific NO_x-emissions. The quality of these signals is hard to rate and strongly depends on engine installation and operation. The uncertainty related to exhaust mass flow is, for example, lower when the engine runs at constant speed and stable load conditions. CAN-bus information of engine load usually represents indicated power. For the calculation of brake-specific emissions, shaft power would be needed. Some vessels are equipped with torque meters measuring the torque of the propeller shaft. The power output of auxiliary engines may be determined based on electrical output. If this information is available onboard, its usage in NO_x monitoring is strongly recommended.

Unfortunately, the effects of long-term monitoring on sensor performance could not be studied due to a lack of data. Previous studies [8] showed that ageing of sensors which were designed for automotive applications is accelerated when they are exposed to the exhaust gas of marine engines. This effect can be attributed to the high temperatures and comparably high levels of particles and soot. Whilst the reduced lifetime was clearly shown in these studies, no conclusions on the accuracy over lifetime were made.

References

[1] T. Frateur, V. E. Verhagen, and F. Kunz, 'Green Deal Validation Study: NOx-CEMS', TNO 2026 R10361, Feb. 2026.

[2] *Commission Delegated Regulation (EU) 2017/655 of 19 December 2016 supplementing Regulation (EU) 2016/1628 of the European Parliament and of the Council with regard to monitoring of gaseous pollutant emissions from in-service internal combustion engines installed in non-road mobile machinery (OJ L 102, 13.4.2017, p. 334)*. 2016. Accessed: Oct. 03, 2025. [Online]. Available: https://eur-lex.europa.eu/legal-content/EN/TXT/?uri=CELEX:02017R0655-20221228

[3] *Commission Delegated Regulation (EU) 2017/654 of 19 December 2016 supplementing Regulation (EU) 2016/1628 of the European Parliament and of the Council with regard to technical and general requirements relating to emission limits and type-approval for internal combustion engines for non-road mobile machinery (OJ L 102, 13.4.2017, p. 1)*. 2016. Accessed: Oct. 03, 2025. [Online]. Available: https://eur-lex.europa.eu/legal-content/EN/TXT/?uri=CELEX:02017R0654-20210913

[4] *Regulation (EU) 2016/1628 of the European Parliament and of the Council of 14 September 2016 on requirements relating to gaseous and particulate pollutant emission limits and type-approval for internal combustion engines for non-road mobile machinery, amending Regulations (EU) No 1024/2012 and (EU) No 167/2013, and amending and repealing Directive 97/68/EC (OJ L 252, 16.9.2016, p. 53)*. 2016. Accessed: Oct. 03, 2025. [Online]. Available: https://eur-lex.europa.eu/legal-content/EN/TXT/?uri=CELEX:02016R1628-20220717

[5] *NEN-ISO 8178-1:2020, Reciprocating internal combustion engines - Exhaust emission measurement - Part 1: Test-bed measurement systems of gaseous and particulate emissions*, Jul. 2020.

[6] *NEN-ISO 8178-4:2020, Reciprocating internal combustion engines - Exhaust emission measurement - Part 4: Steady-state and transient test cycles for different engine applications*, Jul. 2020.

[7] *Uncertainty of measurement — Part 3: Guide to the expression of uncertainty in measurement (GUM:1995)*, 98–3, 2008.

[8] J. Weisheit *et al.*, 'THE SCIPPER PROJECT - Shipping Contributions to Inland Pollution Push for the Enforcement of Regulations', D1.6 Conclusions of technical possibilities of onboard sensor monitoring, Sep. 2022.

Signature

TNO Mobility & Built Environment The Hague, 18 February 2026

Fieke Beemster
Research manager

P. Paschinger
Author

Appendix A
Supplementary information

A.1 Files obtained from Multronic

- 009.105.009-00 009 Sensor NOx C 3012 ppm E A 24VDC C M20 - J1939 (GEN 2) Datasheet Rev01_DEC.pdf
- Main results from IDIADA report No. LM2112 (IDIADA Automotive Technology SA)
- E56 - D2 + NTE official homologation
  - E56 - D2 - 6M26.3-V.pdf
  - E56 D2 + NTE 2022.01.13 Official Homologation - TNO.log
  - E56_M1.txt
  - E56_M2.txt
  - E56_M3.txt
  - E56_M4.txt
  - E56_M5.txt
  - E56_NTE-11.txt
- Test bench data Multronic CEMS
  - E3 cycle + NTE_.pdf
  - DE-Tronic E43 - E3&NTE
  - E43_M1.txt
  - E43_M2.txt
  - E43_M3.txt
  - E43_M4.txt
  - Random-1.txt
  - Random-2.txt

A.2 Constants used in calculations

Table 4.1: Constants used for calculation.

Symbol	Description	Value	Unit	Reference
ρ_{air}	Density of air at 273.15 K and 101.325 kPa	1.293	kg/m^3	[3]
ρ_{diesel}	Density of diesel at 15°C	849.0[4]	kg/m^3	[3]
ρ_{exh}	Density of diesel exhaust gas at 273.15 K and 101.325 kPa	1.2943	kg/m^3	[3]
DF_{NOx}	Multiplicative deterioration factor for NO_x	1.15	1.0	IDIADA report No. LM2112
u_{CO}	Component specific factor or ratio between densities of gas component and exhaust gas (CO)	0.000966	1.0	[3]
u_{CO2}	Component specific factor or ratio between densities of gas component and exhaust gas (CO_2)	0.001517	1.0	[3]
u_{NOx}	Component specific factor or ratio between densities of gas component and exhaust gas (NO_x)	0.001586	1.0	[3]

[4] This number represents the average of minimum and maximum values stated in the reference document.

A.3 Condition numbers of SD-method

Equation A.1: Relative condition numbers of SD-method.

$$\kappa_{\mathrm{rel},n} = \frac{\left|\eta_{\mathrm{vol}} \cdot f \cdot V_{\mathrm{disp}} \cdot \frac{1}{60} \cdot \frac{273.15}{\mathrm{MAT}+273.15} \cdot \frac{\mathrm{MAP}}{1.01325}\right|}{\left|\eta_{\mathrm{vol}} \cdot f \cdot V_{\mathrm{disp}} \cdot \frac{n}{60} \cdot \frac{273.15}{\mathrm{MAT}+273.15} \cdot \frac{\mathrm{MAP}}{1.01325}\right|} \cdot |n| = \frac{|n|}{|n|} = 1.0$$

$$\kappa_{\mathrm{rel},\eta_{\mathrm{vol}}} = \frac{\left|f \cdot V_{\mathrm{disp}} \cdot \frac{n}{60} \cdot \frac{273.15}{\mathrm{MAT}+273.15} \cdot \frac{\mathrm{MAP}}{1.01325}\right|}{\left|\eta_{\mathrm{vol}} \cdot f \cdot V_{\mathrm{disp}} \cdot \frac{n}{60} \cdot \frac{273.15}{\mathrm{MAT}+273.15} \cdot \frac{\mathrm{MAP}}{1.01325}\right|} \cdot |\eta_{\mathrm{vol}}| = \frac{|\eta_{\mathrm{vol}}|}{|\eta_{\mathrm{vol}}|} = 1.0$$

$$\kappa_{\mathrm{rel},MAP} = \frac{\left|\eta_{\mathrm{vol}} \cdot f \cdot V_{\mathrm{disp}} \cdot \frac{n}{60} \cdot \frac{273.15}{\mathrm{MAT}+273.15} \cdot \frac{1}{1.01325}\right|}{\left|\eta_{\mathrm{vol}} \cdot f \cdot V_{\mathrm{disp}} \cdot \frac{n}{60} \cdot \frac{273.15}{\mathrm{MAT}+273.15} \cdot \frac{\mathrm{MAP}}{1.01325}\right|} \cdot |\mathrm{MAP}| = \frac{|\mathrm{MAP}|}{|\mathrm{MAP}|} = 1.0$$

$$\kappa_{\mathrm{rel},MAT} = \frac{\left|\eta_{\mathrm{vol}} \cdot f \cdot V_{\mathrm{disp}} \cdot \frac{n}{60} \cdot \frac{-\mathrm{MAT}}{(\mathrm{MAT}+273.15)^2} \cdot \frac{\mathrm{MAP}}{1.01325}\right|}{\left|\eta_{\mathrm{vol}} \cdot f \cdot V_{\mathrm{disp}} \cdot \frac{n}{60} \cdot \frac{273.15}{\mathrm{MAT}+273.15} \cdot \frac{\mathrm{MAP}}{1.01325}\right|} \cdot |\mathrm{MAT}|$$

$$= \frac{\left|\frac{\mathrm{MAT}}{(\mathrm{MAT}+273.15)^2}\right| \cdot |MAT|}{\frac{273.15}{\mathrm{MAT}+273.15}} = \frac{|MAT|}{|\mathrm{MAT}+273.15|} < 1.0$$

A.4 Test setup

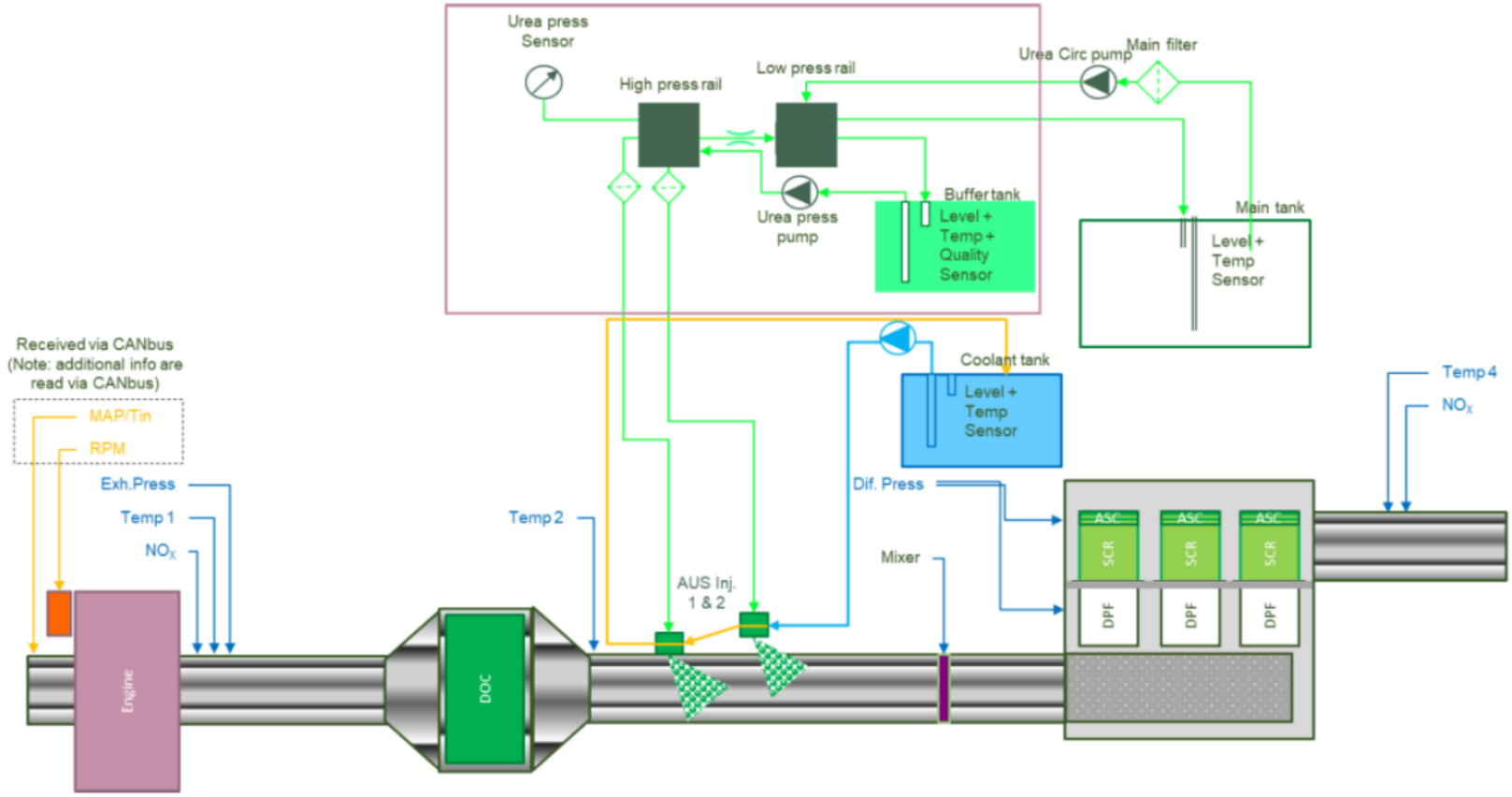

Figure 4.1: Sketch of sensor setup with labels [obtained from Silvano Pautasso (Multronic) on July 14th, 2025, via Microsoft Teams chat].

Mobility & Built Environment

Anna van Buerenplein 1
2595 DA Den Haag
www.tno.nl

TNO innovation for life